

# Faulting Parameters of the September 25, 1998 Pymatuning, Pennsylvania Earthquake

Monica Maceira, Charles J. Ammon, and Robert B. Herrmann

Saint Louis University

## Abstract

On September 25, 1998 a moderate-size ( $m_{bLg}$  5.2) earthquake occurred in northwestern Pennsylvania, near the Ohio border. Source analyses suggested an unusual, non double couple component to the faulting mechanism; but subsequent checks of the near real-time solutions suggested the non double couple component may have been an artifact. We investigate the size of the non double couple faulting component, improve mechanism and depth estimates for the Pymatuning event, and explore the reason(s) why early estimates contained large non double couple source components. We conclude that the non double couple component, while possible, is unnecessary and it can be interpreted as a consequence of small amplitude features in near-nodal Rayleigh waves. We show that the Pymatuning earthquake can be explained with a pure double couple faulting mechanism, corresponding to a near-vertical, mostly strike-slip fault with planes striking  $110^\circ$  and  $13^\circ$ , with dips of  $70^\circ$  and  $71^\circ$ , and rakes of  $20^\circ$  and  $159^\circ$ . The estimated moment is  $5.6 \times 10^{22}$  dyne-cm ( $M_w = 4.5$ ). Regional waveforms constrain the depth of the event to be shallower than 7.5 km, and a short period teleseismic P-waveform from northwest Russia suggests a shallower 2-4 km source. The roughly east-west or north-south striking vertical strike-slip mechanism agrees well with existing estimates of the stress field, and is similar to the 1986 eastern Ohio earthquake mechanism.

# Introduction

Tectonic activity driven by plate interactions can extend far from plate boundaries where most of the seismic activity takes place, and even in the geologically quiet zones, “stable” is a relative term. Hundreds of events worldwide have taken place in what is considered stable continental crust. Small magnitude midplate seismicity is common in the central and eastern North America although, for the most part, the seismicity rate in the central and eastern United States is low compared to that in more seismically active regions such as California and Alaska (Nuttli, 1981). And although earthquakes are rare in eastern North America, the common belief is that their potential for damage is significant because of the low attenuation of seismic wave energy in the frequency range of damaging ground motion. Seismic waves will be felt, and cause damage, over a much larger region in the eastern United States than would waves from a similar magnitude in regions such as California, where attenuation is much greater (Nuttli, 1973; Mitchell, 1973, 1975). On the other hand, some recent studies (Hanks and Johnston, 1992; Bollinger et al., 1993) argue this issue.

In recent years many areas in the stable continental region have been instrumented with networks of modern, digital seismographs. One advantage of the modern instrumentation is the ability to model and assess quickly the impact of earthquakes in near real-time. Such studies of faulting provide important information for the early response (scientific and emergency) to the events.

In 1998, initial, rapid analyses of seismic waveforms generated by the  $m_{bLg}$  5.2 Pennsylvania-Ohio border region earthquake suggested an unusual, non double-couple component to the faulting mechanism (Ekström, personal communication, 1998). Subsequent checks of the near real-time solution suggested that the non double couple component may have been an artifact caused by the available data coverage.

In this paper, we describe our investigation of the Pymatuning earthquake. We used waveform modeling to constrain faulting parameters (source depth, fault strike, dip, and

slip) and to explore the reason(s) why initial moment tensor estimates contained large non double couple source components. We utilized complete seismograms recorded within a few hundred kilometers to the source (including both body and surface-waves) to model the faulting mechanism. We performed inversions for a general, deviatoric moment tensor, and for a pure double couple dislocation source.

## The Pymatuning earthquake

The Pymatuning earthquake occurred in northwestern Pennsylvania on Friday, September 25, 1998, at 19:52:52 UTC . The earthquake epicenter was located by the National Earthquake Center (NEIC) at  $41.5^{\circ}\text{N}$ ,  $80.4^{\circ}\text{W}$ , close to the Ohio-Pennsylvania border. The maximum intensity was VI at communities in Pennsylvania and Ohio (USGS reports); and although the Pymatuning earthquake did not produce a high level of damage to buildings and other human-made structures, the hydrologic effects were a costly result of the event (Armbruster J., et al. (material available online at WWW sites maintained by the US Geological Survey)).

This earthquake is significant for two reasons. First, its magnitude ( $m_{bLg} = 5.2$ ) is the largest for any previous Pennsylvania earthquake. Second, it occurred in an area that only rarely experiences such events. Most prior Pennsylvania earthquakes of moderate magnitude occurred in or near Lancaster County in southeastern Pennsylvania (Armbruster and Seeber, 1987). The largest, recent previous earthquake in the region was the magnitude ( $m_b$ ) 5.0 Leroy (northeastern Ohio) earthquake that occurred on January 31, 1986, about 65 km west-northwest of the Pymatuning shock. Three prior earthquakes occurred in the same epicentral area with magnitudes greater than 3.0 (Seeber and Armbruster, 1993): two were instrumentally located near Pymatuning earthquake, and the third event in 1852 is assumed to have occurred 20-30 km to the northeast.

Two hypotheses have been proposed to explain this intraplate seismicity: (a) selective

reactivation of preexisting faults by local variations in pore pressure, fault friction, and/or strain localization along favorably oriented lower crustal ductile shear zones formed during earlier deformation (Zoback et al., 1985); (b) local stress perturbation which may produce events incompatible with the regional stress field (Zoback et al., 1987). Earthquakes in Pennsylvania region, like most of the seismicity east of the Rocky Mountains, usually occur along preexisting zones of weakness in Precambrian rocks (Seeber and Armbruster, 1993).

Northwestern Pennsylvania is part of the Appalachian Plateaus province which extends from Alabama northeastward into New York. This province in Pennsylvania is divided into seven sections, and the Pymatuning event took place in the Glaciated Pittsburgh Plateau section. The predominant bedrock stratigraphy in this section is made up by Pennsylvanian Allegheny and Pottsville Formations (cyclic sequences of sandstone, red and gray shale, conglomerate, clay, coal, and limestone), Mississippian Shenango Formation and subjacent rocks (red and gray sandstone, shale, and limestone), and upper Devonian Riceville Formation and Venango Group (red sandstone, gray shale, black shale, limestone, and chert) (generalized geologic map of Pennsylvania, Pennsylvania Geological Survey, 1990). The geologic structure at the surface is, in general, very gentle south dip with minor irregularities (Beardsley, et al., 1999). The formation of this landscape began in the late Paleozoic Alleghanian orogeny which created a high mountain chain to the southeast of the present plateaus. Sediments were carried from this mountain chain northwestward or northward across Pennsylvania. During the Triassic and Jurassic, with the opening of the Atlantic basin and consequent creation of new steep stream gradients eastward, the highlands in eastern Pennsylvania were eroded. The erosion rates were great during latest Paleozoic and Mesozoic, but they were much slower during the Cenozoic. About 70 million years ago, the plateaus had already their general shape and size. Finally, Pleistocene glaciation completed the morphology with considerable modifications to plateau drainage (Briggs, 1999). As a result of all these factors, the general aspect of the Glaciated Pittsburgh section of the Appalachian Plateaus province is one of rolling, subparallel ridges generally oriented south-southeast, wandering

streams, and large and small marshes and other bodies of water. Few faults have been recognized at the surface in this region. Wegweisser et al. (1998) suggested that seismicity in NW Pennsylvania may be associated with the NW trending “cross-strike discontinuities” in the Precambrian basement. Alexandrowicz and Cole (1999) found evidence of preexisting NW striking faults in the epicentral region of the Pymatuning shock and suggested that the earthquake may have occurred on a reactivated Precambrian basement structure that trends northwest-southeast and dips steeply to the northeast.

## Seismic Observations

The Pymatuning earthquake was well recorded by both the US and the Canadian National Seismic Networks. We examined waveforms recorded by these three-component, broadband seismic networks, but only 13 of the closest stations were used in this study (Figure 1 and Table 1). A careful examination of the observations is an important part of investigating the significance and cause of the unusual, non double couple source suggested by the initial analyses of the waveforms generated by the Pymatuning earthquake. Although corrupt data are not the cause of the source complexity, a number of interesting observations on instrument performance are possible.

Careful examination of the raw vertical (velocity) component traces revealed a nonlinear component to signals at BINY, BLA and GAC. Specifically, soon after the S-arrival, a broad trough initiated and continued for at least another minute. The cause of these signals is uncertain and difficult to pin down without detailed instrument information. The initiation of the problematic response with the large-amplitude S-waves suggests that the problem may have been electronic saturation (for a complete list of stations with possibly nonlinear instrument problems see Maceira, 2000). However the original signals do not show clear evidence of clipping, only the broad nonlinear signal. The potential problems associated with the clipping could have important consequences on the performance of the national

networks in the event of a large earthquake in the east. We also noted a polarity problem on the GWDE east component, which may be present on data recorded through 1999.

## The Pymatuning earthquake moment-tensor

Regional distance analysis is extremely important in the study of small or moderate-sized earthquakes ( $m_b \leq 5.5$ ), which are rarely well recorded at teleseismic distances (e.g. Dreger and Helmberger, 1990, Dreger et al., 1995, Romanowicz et al., 1993, Ammon et al., 1998). To estimate the moment tensor of the Pymatuning earthquake we modeled the complete waveforms recorded at the closest stations in the period range between 50 and 10 seconds, depending on the epicentral distance. We used complete synthetic seismograms calculated using Kennett's (1983) reflection-matrix method as implemented by G. E. Randall (1994), and aligned the observed and the synthetics on the first P arrival time to minimize dependence on structure. Alignment reduces problems with location, origin-time uncertainty, and absolute velocity differences between the earth and the chosen velocity model (e.g. Ammon et al., 1998). We assumed a step source time function which is consistent with the small event size and the periods we model. The crustal model used in the inversion is a five-layer model developed by Herrmann (1979) for the central United States. Although derived for the central US, this model proved adequate to model regional waveforms of the 1994 Wyomissing Pennsylvania earthquake (Ammon et al., 1998).

### *Least-squares time-domain inversion*

We first performed least-squares, time-domain inversions of the complete waveforms to estimate the optimal moment tensors for depths between 2.5 and 25 km. Seismograms from six stations with epicentral distances less than 500 km (BINY, BLA, GWDE, MCWV, SADO, SSPA) were included in the initial inversion. Then we added another six stations (CCM, GOGA, HRV, JFWS, KAPO, LBNH) with epicentral distances between 500-1000 km to test

the match between observed and synthetic seismograms, which remained good.

The match between observations and synthetics is measured by the sum of the square difference between the observed and predicted seismograms, divided by the sum of all observed square seismogram amplitudes.

The resulting match between observations and synthetics is reasonably good for depths between 2.5 and 7.5 km (see Table 2). Similar to previous analyses, these moment tensor inversion results suggest that the source of the Pymatuning earthquake is not a pure double couple. The compensated linear vector dipole (CLVD) ratio  $f_{clvd}$  measures how different the source is from a pure double couple source. For a pure double couple source,  $f_{clvd}$  is zero, while  $f_{clvd}$  is  $\pm 0.5$  for a pure CLVD source. The clvd ratio for the Pymatuning earthquake (depth = 5.0 km) is - 0.38 which means that the moment tensor is 76% non double couple. The estimated moment is  $5.6 \times 10^{22}$  dyne-cm, which corresponds to a moment magnitude of 4.5. The major double couple planes strike at 14 N and 110 N, with dips of  $77^\circ$  and  $67^\circ$ , and rakes of  $156^\circ$  and  $15^\circ$ . The P axis strikes 63 N and plunges  $7^\circ$ , the tension axis strikes 330 N and plunges  $26^\circ$ . These results are consistent with previous studies of the stress regime in central and eastern United States (Zoback, 1992).

The waveform fits computed by assuming a source depth of 2.5 km are shown in Figure 2. A solid line indicates the observations, a dashed line, the predictions. The three components of each station are shown with a uniform amplitude scale. A number of waveforms were not used in the inversion but predicted waveforms are computed and displayed for completeness (vertical BINY, and radial BLA, GOGA and JFWS). For stations farther than 500 km, the fits are surprisingly good: the observations and predictions are slightly out of phase but the main features such as the relative amplitudes of Rayleigh, Love, and body waves are reproduced well. More specifically, the Rayleigh and Love waves are comparable in size at BINY, CCM, HRV, and KAPO, but the Love wave dominates at BLA, GWDE, JFWS, MCWV, SADO, and SSPA, and the Rayleigh waves dominate at station LBNH. Body waves are small at the distant stations but  $P_{nL}$  waves are clearly visible at BINY, HRV, and LBNH.

Event depth is best constrained by Rayleigh waves which show substantial sensitivity to this aspect of the source. Although most information on shallow sources is at periods shorter than we can fit with simple earth models, the intermediate period waveforms do constrain the source depth to be less than 7.5 km, and more likely less than five. Later we use a teleseismic body wave to corroborate this observation and to show the shallower depth is more appropriate for the Pymatuning event.

Lower hemisphere focal mechanisms for the full moment tensor for a depth of 5 km and two equivalent tensor decompositions are shown in Figure 3. The major and minor double couple non-unique decomposition used in this study is shown in the second row. The major double couple is a strike slip mechanism with the same P and T axes as the main event. The minor double couple is about 40% smaller. The change in stress directions from major to minor double couples is somewhat problematic when trying to interpret a non-double couple source as a multiple event. An alternative decomposition that preserves the compressional direction (Wallace, 1985, Julian, 1998, Villagomez, 1999) (a feature appealing in ENA) is shown in the bottom row. The mechanisms consist of a slightly smaller version of the major DC and a suitably oriented reverse fault (strike of 180, dip of 45, rake of  $129^\circ$ ).

Each of the moment tensor decompositions in Figure 4 is equivalent and consistent with the full moment tensor. However, before interpreting the apparent source complexity in terms of multiple ruptures, we must carefully and thoroughly investigate the significance of the exotic source component. Can we explain the observations with a simpler source? Are certain outlier observations producing the non-double couple component in the source?

### ***L1 norm time-domain inversion***

The results from the least-squares, time-domain moment tensor inversion fit the observed waveforms properly, but the percentage of non double-couple component to the faulting mechanism is very high (76%). One hypothesis is that some observations are outliers and

that they are producing this high percentage of non double-couple. To test this hypothesis, we performed the inversion using an L1 norm, which is less sensitive to outliers. We used the complete observed seismograms from the same twelve stations, in the same bandwidth and with the same inversion weight.

These results also produce a good fit to the observations (see Table 3) and a smaller, but still large, percentage of non double-couple component to the faulting mechanism (57%). These results are very similar to the least-squares estimate and so they are also consistent with previous studies of the stress regime in the area. The estimated moment is  $5.2 \times 10^{22}$  dyne-cm, which corresponds to a moment magnitude of 4.4. The major double couple planes strike at 15 N and 109 N, with dips of  $77^\circ$  and  $75^\circ$ , and rakes of  $165^\circ$  and  $13^\circ$ . The P axis strikes 62 N and plunges  $1^\circ$ , the tension axis strikes 332 N and plunges  $19^\circ$ .

Once again, the match between observed and predicted waveforms is not perfect, but the main features are fit well. The moment tensor closely resembles the least squares estimate with a similar radiation pattern and a slightly smaller non-double couple component. As expected, the decompositions produce results similar to that of the least-squares analysis.

These results indicate that the high percentage of non double-couple component to the faulting mechanism is not produced by gross outliers. To check if the observations from a specific station are causing the non double-couple component, we performed separate inversions excluding, one at a time, one of the closest stations. The results show clearly that waveforms at no single station are producing a high percentage of the non double-couple source.

## The dislocation angle grid search

We can use another test to investigate the significance of the non double couple component of the source - a grid search inversion that allows only pure double couples. The grid search is a systematic search for the optimal strike, dip, rake, and moment. We searched all possible

combinations of strike ( $10^\circ$  -  $360^\circ$  with intervals of  $10^\circ$ ), dip ( $0^\circ$  -  $90^\circ$  with intervals of  $10^\circ$ ), and rake ( $-170^\circ$  -  $180^\circ$  with intervals of  $10^\circ$ ). We compute an optimal moment for each dislocation. We performed a separate grid search for each depth between 2.5 km and 25 km with intervals of 2.5 km, and again the match to the observed seismograms is good (see Table 4). The best fit from the grid search for the Pymatuning event is a near-vertical, mostly strike-slip fault at a shallow depth between 2.5 and 7.5 km (see Figure 4). The fault planes for this mechanism strike 110 N and 13 N, with dips of  $70^\circ$  and  $71^\circ$ , and rakes of  $20^\circ$  and  $159^\circ$ . The estimated moment from the grid search at 5.0 km depth is  $5.6 \times 10^{22}$  dyne-cm, which corresponds to a moment magnitude of 4.5. The mechanism resembles the major double couples from the moment tensor inversions.

The waveform fits computed by assuming a source depth of 2.5 km are shown in Figure 4. The fits are comparable to those obtained from the least-squares, time-domain moment tensor inversion. In fact the non double couple moment tensor does not fit the observations significantly better. The “improvement” in fit for non double couple source occurs on the nodal surface waves (BLA, GOGA, GWDE, JFWS, MCWV, SADO, and SSPA) which are small and possibly contaminated by noise and multipathing. We conclude that the non double couple component, while possible, is unnecessary and a consequence of small amplitude features in near-nodal Rayleigh waves.

## Improving the source depth estimate

All three inversions performed in this study match the observed seismograms well for a source depth less than 7.5 km. The best “formal” fit is for the shallowest source, but the 5.0 and 7.5 km depths fit the data well. A summary of waveform misfit is shown in Figure 5. To facilitate the comparison of the L1 and L2 norms, only the L2 misfit is shown (even though the L1 moment tensor inversion and the grid search minimized the L1 norm). Also in Figure 5 we see the stability of the focal mechanism: regardless of the chosen depth, the

focal mechanism changes little. The shallowest source (2.5 km for instance) is closest to a pure double couple (also Table 2).

To better constrain the depth, we used a teleseismic P-waveform observation from station YAK, Yakutsk, Russia. Other P waveforms were examined but proved too noisy (not unusual for a small, near-vertical strike-slip event). The teleseismic body waves are relatively simple, dominated by the direct and primary surface reflections. We can use the relative timing of the depth phases to choose the best source depth. Synthetics were calculated with a uniform crust with a P-velocity of 6.2 km/s. Visual comparison of the observations and predictions (see Figure 6) clearly indicates a shallow source, probably near 2.5 km, but conservatively between 2.5 and 5.0 km depth. Sediment thickness in the region is approximately 2-3 km (World Mapping Project from Exxon Production Research Company, Basin Exploration Division, Basin Analysis Section, 1985). Thus the YAK observations suggest that the source was located near the top of the crystalline basement. If the event is above the basement, it is an unusual occurrence in this region where seismicity usually takes place along preexisting weak zones in Precambrian rocks (Seeber and Armbruster, 1993).

## Conclusions

Initial near real-time analysis of seismic waveforms generated by the  $m_{bLg}$  5.2, September 25, 1998 Pennsylvania-Ohio border region earthquake suggested an unusual, large size, non double couple component to the faulting mechanism. Our analysis showed that the non double couple can be interpreted as resulting from small features in near-nodal Rayleigh waves and can be considered an artifact.

Although both the unusual moment tensor and pure double couple fit the regional waveforms well, the preferred solution in this study is the shear dislocation for three main reasons. First, the solution is in agreement with existing estimates of the stress field (E-W, NE-SW compression) in the region (Zoback, 1992, Figure 7 with exception of the 11/20/69 event).

Second, the dislocation angles are consistent with the January 31, 1986 Ohio earthquake faulting mechanism (figure 7). And third, the Pymatuning earthquake was a small earthquake, and most likely a simple event. Our analysis suggests that the fault planes strike 110 N and 13 N, with dips of  $70^\circ$  and  $71^\circ$ , and rakes of  $20^\circ$  and  $159^\circ$ . The estimated moment from the grid search is  $5.6 \times 10^{22}$  dyne-cm, which corresponds to a moment magnitude of 4.5. The faulting parameters (strike, dip, and rake) obtained in this study are not in agreement with the suggestion of an earthquake occurring on a structure trending northwest-southeast (Wegweisser et al., 1998, Alexandrowicz and Cole, 1999). Much like the 1986 Ohio event, our results are more consistent with an east-west or north-south trending structure. More careful and detailed studies of the earthquakes in ENA are necessary in order to improve the connections between geology and seismicity, which remain poorly understood.

## Acknowledgments

This study was supported by the USGS Cooperation Agreement 1434-HQ-98-AG-01 941, and DSWA Contract 01-98-C-0160. Thanks to Harley Benz for his help with the data; to George E. Randall for use of his reflectivity codes; to Pöl Wessel and Walter H.F. Smith for their extraordinary map-making tool, Generic Mapping Tools (GMT); and to the U.S. Geological Survey, the Canadian National Seismic Network of the Geological Survey of Canada, and IRIS for their cooperation sharing the data.

# Bibliography

- Alexandrowicz, N., and R. Cole, Structure beneath the Appalachian Plateau of northwestern Pennsylvania and relationship to the 1998 Pymatuning earthquake, Geological Society of America Abstracts with Programs, V31, No. 2, 1999.
- Armbruster J., H. Barton, P. Bodin, T. Buckwalter, J. Cox, E. Cranswick, J. Dewey, G. Fleeger, M. Hooper, S. Horton, D. Hoskins, D. Kilb, M. Maramonte, A. Metzger, D. Risser, L. Seeber, H. Shedlock, K. Stanley, M. Withers, and M. Zirbes, researchers who collaborated with the US Geological Survey for the material available online at WWW sites cited below and maintained by the US Geological Survey.
- Ammon, C.J., R.B. Herrmann, C.A. Langston, and H. Benz, Faulting parameters of the January 16, 1994 Wyomissing Hills, Pennsylvania Earthquakes, Seism. Res. Lett., V69, No.3, 261-269, 1998.
- Armbruster, J.G., and L. Seeber, The 23 April 1984 Martic Earthquake and the Lancaster Seismic Zone in eastern Pennsylvania, Bull. Seism. Soc. Am., V77, 877-890, 1987.
- Beardsley, R.W., R.C. Campbell, and M.A. Shaw, Appalachian Plateaus, in The Geology of Pennsylvania, C.H. Shultz, ed., Pennsylvania Geological Survey and Pittsburgh Geological Society, 1999.
- Bollinger, G.A., M.C. Chapman, and M.S. Sibol, A comparison of earthquake damage areas as a function of magnitude across the United States, Bull. Seism. Soc. Am., V83, 1064-1080, 1993.
- Briggs, R.P., Appalachian Plateaus province and the eastern lake section of the central lowland province, in The Geology of Pennsylvania, C.H. Shultz, ed., Pennsylvania Geological Survey and Pittsburgh Geological Society, 1999.
- Dreger, D.S., and D.V. Helmberger, Broadband modeling of local earthquakes, Bull. Seism. Soc. Am., V80, 1162-1179, 1990.
- Dreger, D.S., J. Ritsema, and M. Pasmanos, Broadband analysis of the 21 September, 1993 Klamath Falls earthquake sequence, Geophys. Res. Lett., V22, 997-1000, 1995.
- Exxon Production Research Company, Basin Exploration Division, Basin Analysis Section, World Mapping Project, 1985.
- Hanks, T.C., and A.C. Johnston, Common features of the excitation and propagation of strong ground motion for North American earthquakes, Bull. Seism. Soc. Am., V82, 1-23, 1992.
- Herrmann, R.B., Surface wave focal mechanisms for eastern North American earthquakes with tectonic implications, J. Geophys. Res., V84, 3543-3552, 1979.
- Johnston, A.C., and L.R. Kanter, Earthquakes in stable continental crust, Scient. Am., 68-75, March 1990.
- Julian, B.R., A.D. Miller, and G.R. Foulger, Non double-couple earthquakes. 1. Theory, Reviews of Geophys., V36, 525-549, 1998.
- Kennett, B.L.N., Seismic wave propagation in stratified media, Cambridge University Press, Cambridge, England, 342 pages, 1983.

- Langston, C.A., Source inversion of seismic waveforms: the Koyna, India, earthquakes of 13 September 1967, Bull. Seism. Soc. Am., V71, 1-24, 1981.
- Lay, T., and T.C. Wallace, Modern Global Seismology, Academic Press, 521 pages, 1995.
- Maceira, M., Faulting Parameters of the September 25, 1998 Pymatuning, Pennsylvania Earthquake, Masters Dissertation, Saint Louis University, St. Louis, MO, 95 pages, 2000.
- Mitchell, B.J., Radiation and attenuation of Rayleigh waves from the southeastern Missouri earthquake of October 21, 1965, J. Geophys. Res., V78, 886-899, 1973.
- Mitchell, B.J., Regional Rayleigh wave attenuation in North America, J. Geophys. Res., V80, 4904-4916, 1975.
- Nuttli, O.W., Seismic waves attenuation and magnitude relations for eastern North America, J. Geophys. Res., V78, 876-885, 1973.
- Nuttli, O.W., The earthquake problem in the eastern United States, Am. Soc. of Civil Engineers, No. 261, 1981.
- Pennsylvania Geological Survey, Generalized Geologic Map of Pennsylvania, 1990.
- Randall, G.E., Efficient calculation of complete differential seismograms for laterally homogeneous earth models, Geophys. J. Int., V118, 245-254, 1994.
- Romanowicz, B., D.S. Dreger, M. Pasmanos, and R. Uhrhammer, Monitoring of strain release in central and northern California using broadband data, Geophys. Res. Lett., V20, 1643-1646, 1993.
- Seeber, L., and J. Armbruster, Natural and induced seismicity in the Lake Erie-Lake Ontario region: reactivation of ancient faults with little neotectonic displacement, Geographie physique et Quaternaire, V47, 363-378, 1993.
- Villagomez, R.A., The 1995 Macas earthquake sequence, Ecuador: Brittle failure of a flower structure, Masters Dissertation, Saint Louis University, St. Louis, MO, 82 pages, 1999.
- Wallace, T.C., A reexamination of the moment tensor solutions of the 1980 Mammoth Lakes earthquakes, J. Geophys. Res., V90, 11171-11176, 1985.
- Wegweisser, M., A. Wegweisser, L. Babcock, and J.A. Harper, Morphotectonic features associated with cross-strike discontinuities in Upper Devonian rocks of northwestern Pennsylvania, Guidebook for the 63rd Annual Field Conference of Pennsylvania Geologists, Oct. 1-3, 15-17, Erie, PA, 1998.
- Zoback, M.D., et al., New evidence on the state of stress of the San Andreas fault system, Science, 238, 1105-1111, 1987.
- Zoback, M.D., W.H. Prescott, and S.W. Kroeger, Evidence for lower crustal ductile strain localization in southern New York, Nature, 317, 705-707, 1985.
- Zoback, M.L., Stress field constraints on intraplate seismicity in eastern North America, J. Geophys. Res., V97, 11761-11782, 1992.

Some of the information used in this study is available online at the following WWW pages:

<http://groundmotion.cr.usgs.gov/pym>

[http://groundmotion.cr.usgs.gov/PYM\\_PA\\_Geo](http://groundmotion.cr.usgs.gov/PYM_PA_Geo)

(maintained by Dr. Ed Cranswick, USGS)

## Table captions

**Table 1.** Seismic stations used in this study.

**Table 2.** Least square moment tensor inversion misfits for different depths. Also moment tensor elements and compensated linear vector dipole ratio ( $f_{clvd}$ ).

**Table 3.** L1 Norm moment tensor inversion misfits for different depths. Also moment tensor elements and compensated linear vector dipole ratio ( $f_{clvd}$ ).

**Table 4.** Grid search misfits for different depths. Also the obtained fault parameters.

## Figure captions

**Figure 1.** Map of North America showing the earthquake (circle) and stations (triangles) used in this study. The stations with possibly nonlinear instrument problems are represented with white triangles.

**Figure 2.** Waveform matches (vertical, radial and transverse from top to bottom) corresponding to the least square moment tensor inversion for 2.5 km depth. The solid line identifies the observations, the dashed line indicates the predictions. The waveforms not used in the inversion (see text) are also displayed for completeness. The three components of each station are shown with an uniform amplitude and time scale. Also shown in the figure is the focal mechanism resulting from this inversion. The azimuth of each station is identified.

**Figure 3.** Non double-couple focal mechanism resulting from the least squares moment tensor inversion. Decomposition of this NDC mechanism into a major and a minor double couple. The second decomposition is performed fixing the P axis. The moment tensor obtained from the L1 norm time-domain inversion closely resembles the least squares estimate, with a similar radiation pattern and a slightly smaller non double couple component.

**Figure 4.** Waveform matches (vertical, radial and transverse from top to bottom) between observed and synthetic seismograms from the grid search assuming a depth of 2.5 km. The solid line identifies the observations, the dashed line indicates the predictions. The waveforms not used in the inversion (see text) are also displayed for completeness. The three components of each station are shown with an uniform amplitude and time scale. Also shown in the figure is the double couple focal mechanism resulting from this inversion. The azimuth of each station is identified.

**Figure 5.** Misfit versus depth for least-squares and grid search inversions. Also plotted are the focal mechanisms obtained for each of these inversions at different depths.

**Figure 6.** Computed body wave seismograms for source depths of 2.5, 5, and 7.5 km. The results clearly show that a source deeper than 5 km is not appropriate for this event. The comparison of the observation and predictions indicates a shallow source, conservatively between 2.5 and 5.0 km depth.

**Figure 7.** Focal mechanisms in Pennsylvania and surrounding states of northeast North America. The Pymatuning event focal mechanism obtained in this study (grey shading for compressional quadrants) is consistent with previous earthquakes in the area.

Sites description					
Station ID	Network	Latitude ( $^{\circ}$ N)	Longitude ( $^{\circ}$ W)	Azimuth ( $^{\circ}$ )	Distance (km)
BINY	USNSN	42.199	75.986	76	382
BLA	USNSN	37.211	80.421	179	473
CCM	USNSN	38.056	91.245	251	996
GAC	CNSN	45.703	75.478	387	622
GOGA	USNSN	33.411	83.467	197	932
GWDE	USNSN	38.826	75.617	124	508
HRV	USNSN	42.506	71.558	78	748
JFWS	USNSN	42.915	90.249	284	822
KAPO	CNSN	49.450	82.508	351	904
LBNH	USNSN	44.240	71.926	63	763
MCWV	USNSN	39.658	79.846	165	208
SADO	CNSN	44.769	79.142	16	385
SSPA	USNSN	40.636	77.888	112	237

TABLE 1

Least Square Moment Tensor Inversion Misfit									
Depth (km)	Misfit (%)	$M_0$ (dyne-cm)	$M_{\theta\theta}$	$M_{\theta\varphi}$	$M_{r\theta}$	$M_{\varphi\varphi}$	$M_{r\varphi}$	$M_{rr}$	$f_{clvd}$
2.5	22.9	5.14E22	-2.31	4.10	0.27	3.50	0.27	-1.19	-0.21
5.0	29.5	5.67E22	-1.61	4.09	-0.07	4.25	1.24	-2.64	-0.38
7.5	29.6	5.79E22	-1.60	4.44	-0.08	4.16	0.78	-2.56	-0.37
10.0	41.3	5.69E22	-1.67	4.36	0.44	4.02	0.96	-2.36	-0.38
12.5	46.3	5.76E22	-1.63	4.55	0.30	3.77	0.84	-2.13	-0.34
15.0	51.5	5.70E22	-1.43	4.81	0.31	3.13	1.35	-1.70	-0.28
17.5	52.1	6.06E22	-1.56	5.26	0.38	3.17	1.19	-1.61	-0.26
20.0	54.2	6.58E22	-1.99	5.43	0.573	4.00	1.22	-2.01	-0.30
22.5	65.7	6.20E22	-1.75	5.25	0.88	3.43	1.10	-1.68	-0.27
25.0	74.5	5.86E22	-0.61	5.15	1.11	2.01	1.83	-1.39	-0.29

TABLE 2

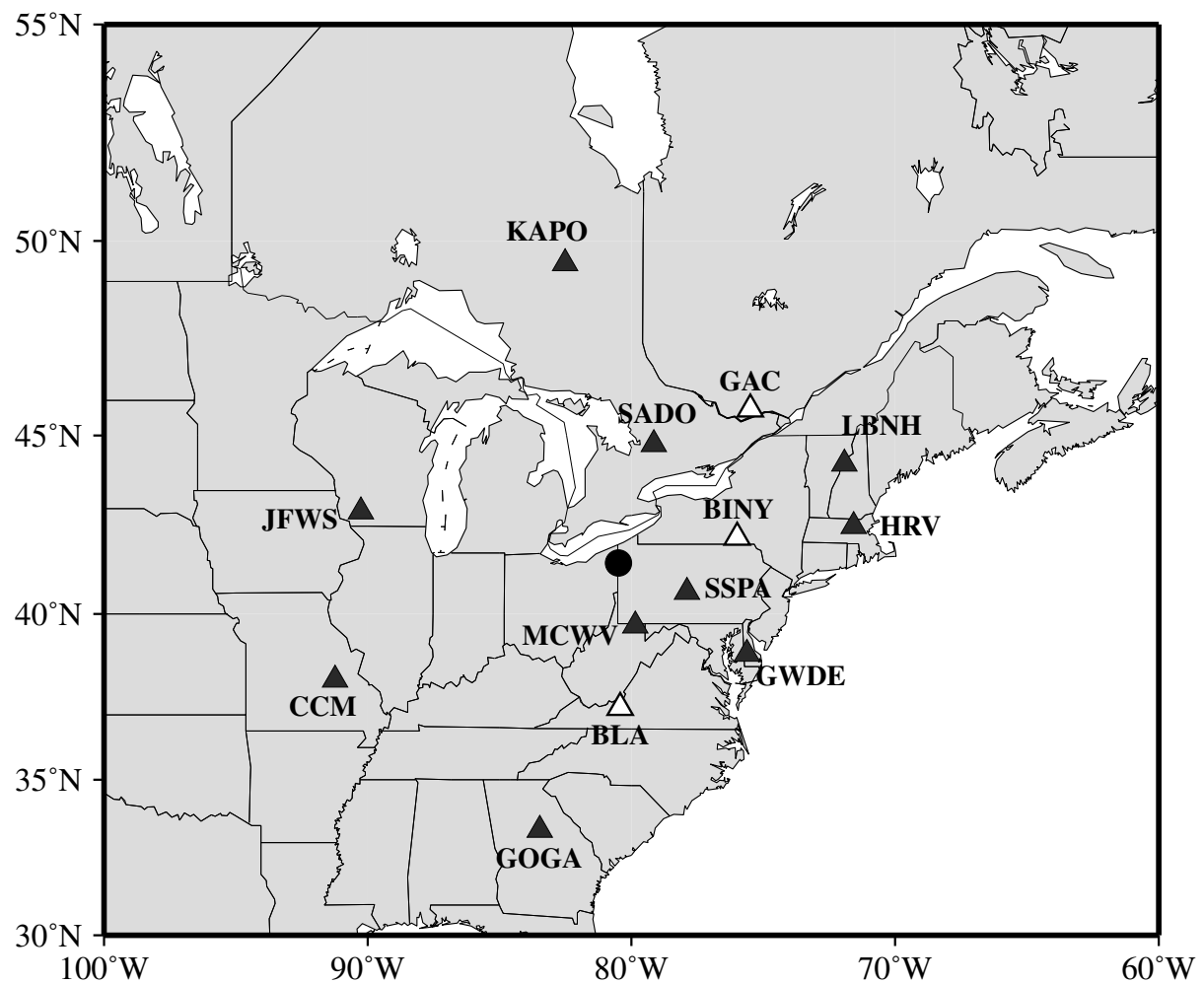
Norm L1 Moment Tensor Inversion Misfit									
Depth (km)	Misfit (%)	$M_0$ (dyne-cm)	$M_{\theta\theta}$	$M_{\theta\varphi}$	$M_{r\theta}$	$M_{\varphi\varphi}$	$M_{r\varphi}$	$M_{rr}$	$f_{clvd}$
2.5	23.4	4.96E22	-2.15	3.95	-0.50	3.21	-0.84	-1.06	-0.22
5.0	30.0	5.23E22	-1.77	4.04	-0.60	3.72	0.52	-1.95	-0.29
7.5	29.8	5.58E22	-1.73	4.43	-0.41	3.83	0.45	-2.11	-0.31
10.0	42.0	5.53E22	-1.75	4.39	-0.36	3.74	0.83	-1.99	-0.29
12.5	47.1	5.98E22	-2.06	4.82	-0.37	3.95	0.79	-1.89	-0.26
15.0	52.3	5.90E22	-1.88	4.85	-0.43	3.64	1.11	-1.76	-0.24
17.5	53.1	5.76E22	-1.83	4.82	-0.40	3.45	0.92	-1.62	-0.23
20.0	55.7	5.71E22	-1.79	4.76	-0.43	3.47	0.86	-1.68	-0.24
22.5	67.5	5.53E22	-1.92	4.61	-0.45	3.29	0.98	-1.37	-0.20
25.0	77.0	4.93E22	-1.31	4.21	-0.47	2.50	1.26	-1.19	-0.17

TABLE 3

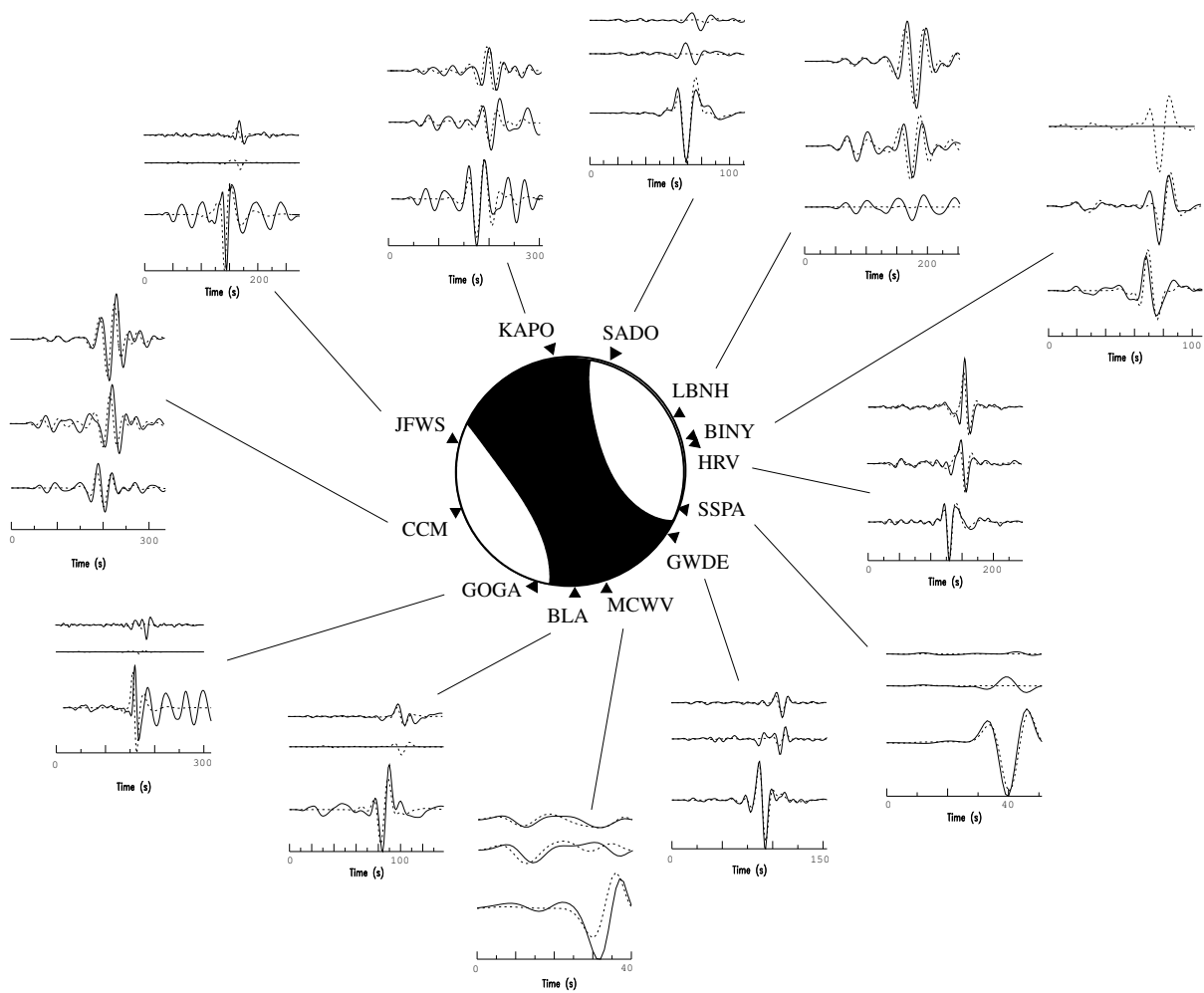
Grid Search Misfit					
Depth (km)	Misfit (%)	$M_0$ (dyne-cm)	Strike ( $^{\circ}$ )	Dip ( $^{\circ}$ )	Slip ( $^{\circ}$ )
2.5	24	5.69E22	110	70	20
5.0	32	5.67E22	110	70	20
7.5	32	5.63E22	110	80	10
10.0	45	5.74E22	110	80	10
12.5	50	5.83E22	10	80	170
15.0	55	6.16E22	10	80	170
17.5	56	6.73E22	10	80	170
20.0	60	7.48E22	110	80	10
22.5	72	7.83E22	110	80	0
25.0	85	8.03E22	20	90	170

TABLE 4

FIGURE 1



**FIGURE 2**



**FIGURE 3**

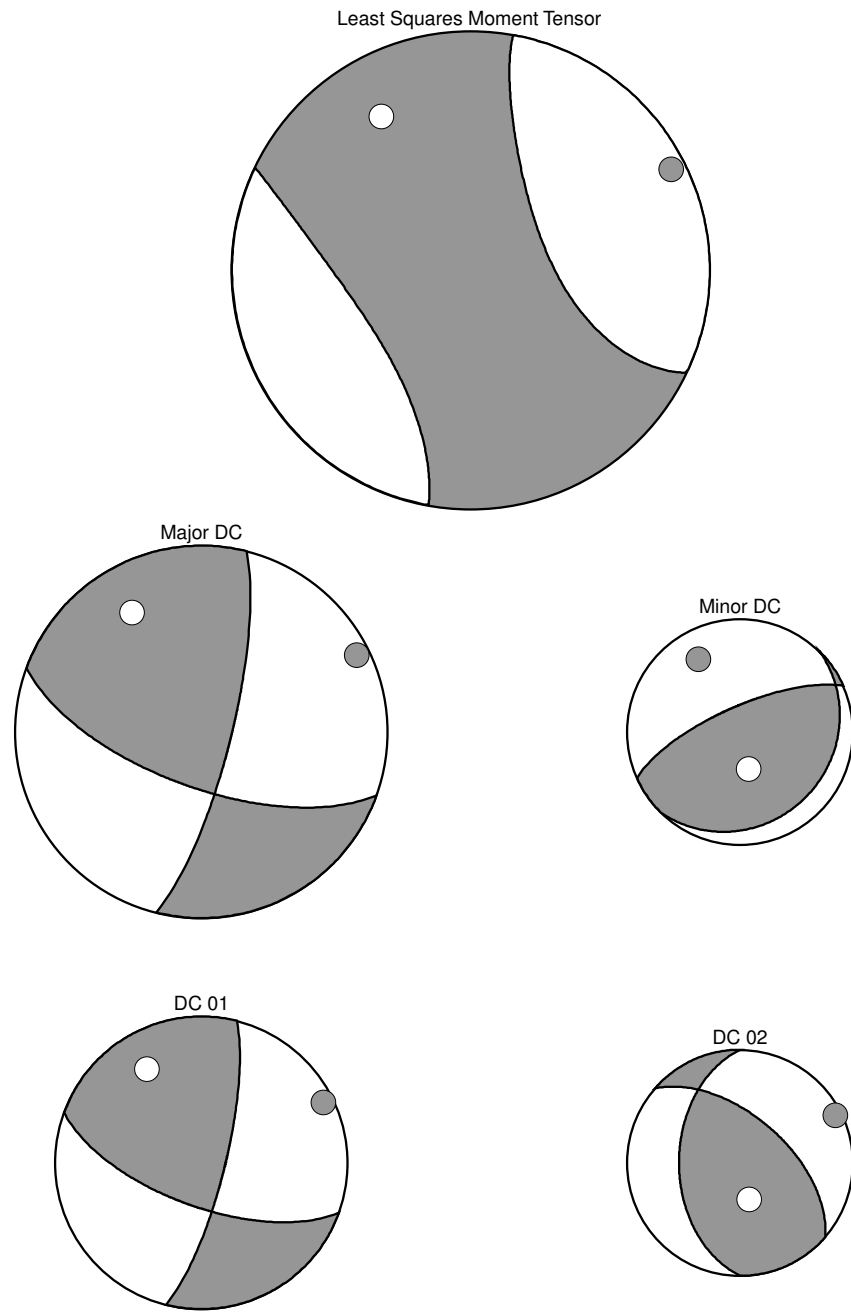


**FIGURE 4**

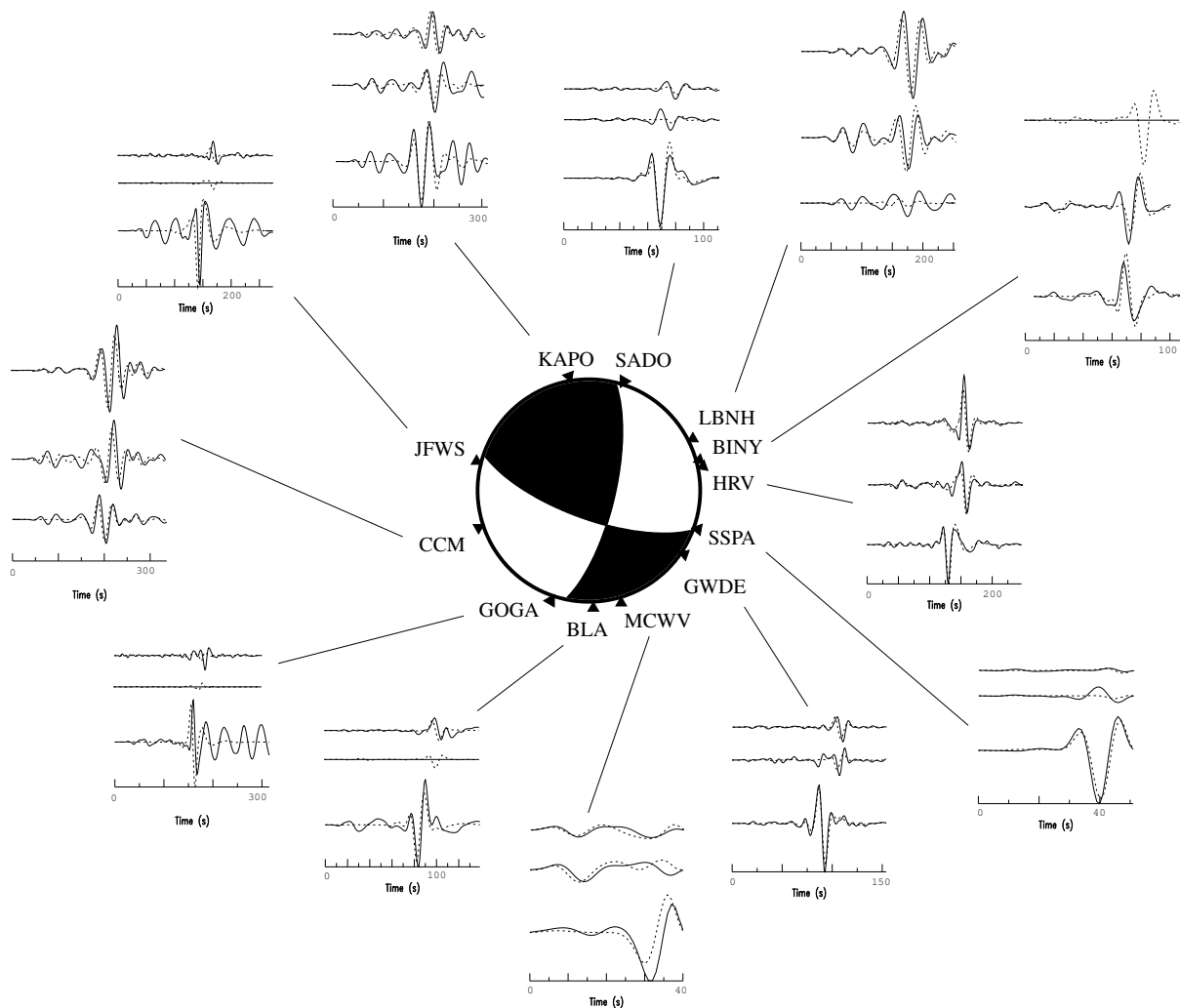


**FIGURE 5**

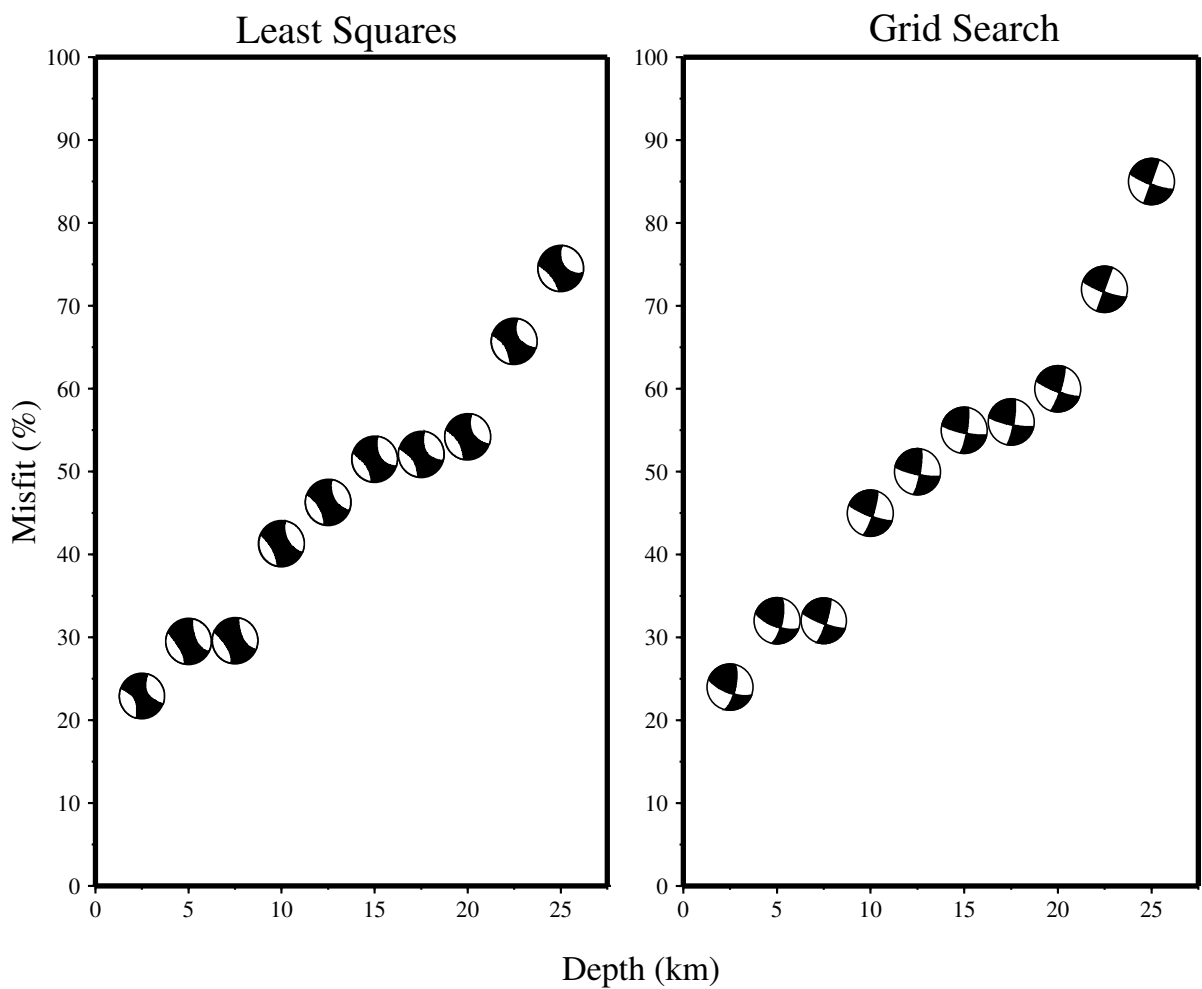
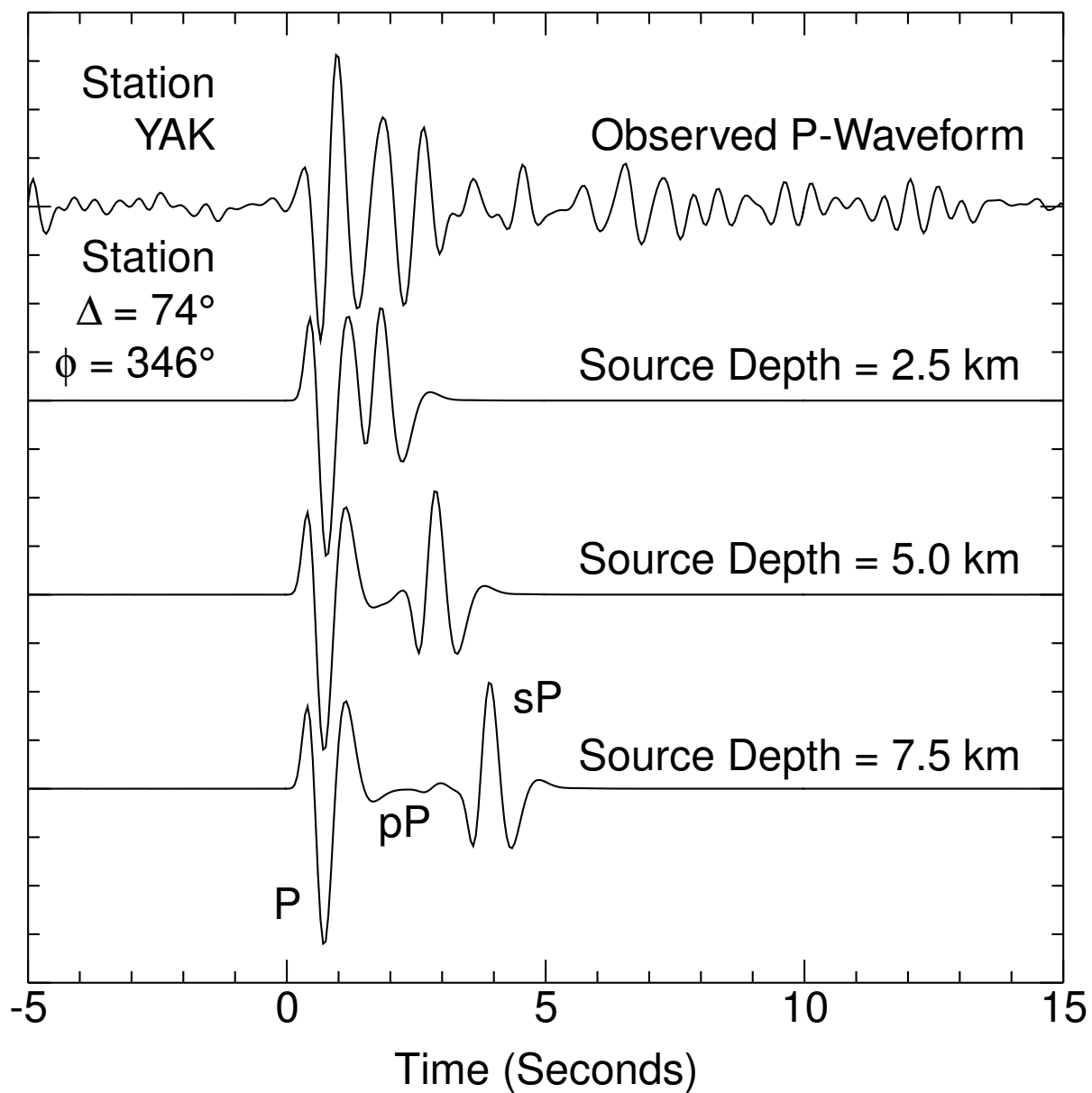


FIGURE 6



**FIGURE 7**

